Seasonal trends in photosynthesis and leaf traits in scarlet oak

Contributor names: Angela C. Burnett*, Shawn P. Serbin, Julien Lamour, Jeremiah Anderson,

Kenneth J. Davidson, Dedi Yang, Alistair Rogers

Address for all authors:

Environmental and Climate Sciences Department

Brookhaven National Laboratory

Upton, New York, USA

Email address of author for correspondence:

acb219@cam.ac.uk

*Present address:

Department of Plant Sciences, University of Cambridge, Downing Street, Cambridge, CB2 3EA, UK

Key words: Gas exchange, leaf traits, phenology, physiology, temporal changes, $V_{c,max}$

Running head: Seasonal trends in scarlet oak

Abstract: 256 words (max. 300)

Introduction: 703 words (max. 1000)

Abstract

Understanding seasonal variation in photosynthesis is important for understanding and modelling plant productivity. Here we used shotgun sampling to examine physiological, structural and spectral leaf traits of upper canopy, sun-exposed leaves in *Quercus coccinea* Münchh (scarlet oak) across the growing season in order to understand seasonal trends, explore the mechanisms underpinning physiological change, and investigate the impact of extrapolating measurements from a single date to the whole season. We tested the hypothesis that photosynthetic rates and capacities would peak at the summer solstice i.e. at the time of peak photoperiod. Contrary to expectations, our results reveal a late-season peak in both photosynthetic capacity and rate before the expected sharp decrease at the start of senescence. This late-season maximum occurred after the higher summer temperatures and VPD, and was correlated with the recovery of leaf water content and increased stomatal conductance. We modelled photosynthesis at the top of the canopy and found that the simulated results closely tracked the maximum carboxylation capacity of Rubisco. For both photosynthetic capacity and modelled top-of-canopy photosynthesis, the maximum value was therefore not observed at the summer solstice. Rather, in each case the measurements at and around the solstice were close to the overall seasonal mean, with values later in the season leading to deviations from the mean by up to 41% and 52% respectively. Overall we found that the expected Gaussian pattern of photosynthesis was not observed. We conclude that an understanding of species- and environment-specific changes in photosynthesis across the season is essential for correct estimation of seasonal photosynthetic capacity.

Introduction

Photosynthesis underpins primary productivity on Earth. Understanding photosynthesis is essential for developing accurate Terrestrial Biosphere Models (TBMs), which aim to represent the responses of plants to future climate and the role plants play in determining the rate of global change. Accounting for temporal and spatial variation in photosynthesis is critical if TBMs are to accurately predict carbon fluxes across space and through time. For example, under-representation of photosynthetic understanding due to an absence of relevant data in certain geographical areas, such as Arctic ecosystems, can lead to significant biases in model predictions (e.g. Rogers et al. 2017). To address the constraint of limited data availability for parameterisation, some TBMs use nitrogen as a proxy for photosynthesis, yet the relationship between nitrogen and photosynthesis has been shown to vary by plant functional type (Kattge et al. 2009) making this challenging. In addition, consideration of seasonal changes is important given that photosynthetic capacity has been shown to display significant variation during the growing season (Wilson et al. 2001, Wang et al. 2008, Bauerle et al. 2012, Ali et al. 2015). Environmental parameters such as photoperiod and growth temperature may explain this seasonal variation in photosynthetic capacity, since climatic conditions have been demonstrated to be a better proxy for photosynthesis than leaf nitrogen (Ali et al. 2015, Smith et al. 2019). For example, a recent study of 23 tree species found that photoperiod was the primary environmental driver for seasonal changes in photosynthetic capacity – both the maximum carboxylation capacity of Rubisco ($V_{c,max}$) and the maximum electron transport rate (J_{max}) (Bauerle et al. 2012). However, the extent to which different environmental conditions underpin photosynthetic rate can vary between species and ecosystems studied, with temperature,

moisture availability and atmospheric humidity being other important environmental factors to consider (Ali et al. 2015).

A–C_i response curves measure the response of photosynthesis (A) to the internal CO_2 concentration inside the leaf (C_i). With these curves it is possible to derive estimates of the apparent maximum carboxylation capacity of Rubisco ($V_{c,max}$) and apparent maximum electron transport rate (J_{max}), two key parameters related to photosynthetic capacity (Long and Bernacchi 2003). However, obtaining accurate measurements of photosynthetic capacity in tree species is not without its challenges. The ideal scenario, performing measurements *in situ* whilst preserving the water column to the leaf and maintaining ambient environmental conditions, requires expensive aerial work platforms such as "cherry-pickers" or canopy cranes (Wu et al. 2019). Lower-cost and more logistically feasible solutions involve retrieving samples from the canopy for subsequent measurement. There exists a range of approaches for retrieving canopy samples, including line launchers, sling shots or air cannons (Serbin et al. 2014); for samples lower in the canopy pruning poles are often sufficient (Kamoske et al. 2020). If retrieval times are lengthy, leading to a long sample collection period, this can result in sample deterioration. The shotgun sampling approach, using a shotgun to retrieve leaf samples (Serbin et al. 2014, Burnett et al. 2019), enables rapid acquisition of plant material from the top of the canopy. Collecting and stabilising each sample takes a matter of minutes, enabling the rapid acquisition of a set of samples within a short time period. This means that all samples may be collected at dawn, before photosynthetic activity begins to acclimate to the day's conditions, and ensures that leaf quality is maintained throughout the measurement period due to the speed of sample collection.

We sought to understand the seasonal variation in physiological and structural leaf traits in *Quercus coccinea* (scarlet oak) in the mid-Atlantic region using the shotgun sampling approach. We performed regular measurements throughout the entire growing season and examined the relationships between physiological traits, structural traits, leaf nitrogen and leaf chlorophyll to (1) understand seasonal trends, (2) explore the mechanisms underpinning physiological change, and (3) investigate the impact of extrapolating measurements made at a single time point when deriving parameters for use in TBMs. In accordance with previous studies (Wilson et al. 2001, Bauerle et al. 2012), we hypothesised that photosynthetic rates and capacities would be greatest at the midsummer solstice (day of year 172) when photoperiod is at its peak, meaning that a midsummer measurement would provide a significant overestimation of mean photosynthesis if used as a model parameter.

Materials and methods

Tree material

Quercus coccinea Muench (scarlet oak) samples were obtained from a mixed pine-oak forest at Brookhaven National Laboratory, Upton, New York, USA (latitude 40.864466, longitude 72.875158, 18 meter elevation). Scarlet oak is a native, deciduous, xerophytic tree with an open, rounded crown (USDA 2019). The study site is part of the Long Island Pine Barrens, characterised by dry sandy soils (Meng et al. 2017). Six trees were selected at the start of the measurement season and labelled with flagging tape to enable repeated measurements. The trees were located in a small geographic area (<30m radius). Each tree selected displayed a mature canopy structure, so that sampling could be repeated for the duration of the experiment with minimal adverse effects.

Meteorological data

Meteorological data were obtained from the Brookhaven National Laboratory meteorological data service (www.bnl.gov/weather/). Solar data were converted to photosynthetically active radiation by multiplying W m^{-2} by 2.1. VPD was obtained from temperature and relative humidity data using the 'Bigleaf' package in R (Knauer et al. 2018).

Shotgun sampling technique

Leaf samples were collected at dawn. Samples from the top of the canopy were retrieved using shotgun sampling (Serbin et al. 2014, Burnett et al. 2019). A 12-gauge Remington 870 Express Pump-Action Shotgun with a modified choke and stainless-steel bird shot was used to retrieve canopy samples (Fig. 1a). Each sample comprised several leaves, and a small amount of connecting woody material (Fig. 1b). The woody stem of each sample was immediately recut under water (within 2min) and was kept in water until the completion of physiological data collection. Samples were kept in individual bottles of water. Once all samples had been collected (typically <1 hour), samples were transferred from the forest to the laboratory for data collection.

Measurement schedule

Data were collected in 2019 throughout the entire growing season of *Q. coccinea*. The first sampling date occurred when leaves were sufficiently expanded for measurement, i.e. within a couple of weeks of leaf flushing, and the last sampling date occurred at the onset of senescence, with leaves turning scarlet on the trees. There were eight sampling dates (Fig. 2), beginning on DOY 149 (late May) and ending on DOY 303 (late October). Gas exchange measurements were collected on seven

of the eight sampling dates; all leaf trait data were collected on each sampling date with the exception of one date for which no relative water content values could be calculated.

Chlorophyll and PRI

For each sample, spectral data were collected using a PSR+ full-range spectroradiometer (Spectral Evolution, Lawrence, Massachusetts, USA) connected to a leaf clip with an internal light source (SVC, Poughkeepsie, New York, USA). Immediately prior to each set of measurements, the spectroradiometer was calibrated using a LabSphere Spectralon® reflectance standard disc (LabSphere, Inc., North Sutton, New Hampshire, USA). Two to three spectral measurements were taken across the adaxial surface of each leaf depending on leaf size, then averaged to give a single spectrum per sample. Chlorophyll was estimated from each spectrum using the Chlorophyll NDI index. The index was derived from using the formula ($R750 - R705)/(R750 + R705$) where R is optical reflectance at the waveband indicated and chlorophyll content was estimated using the conversion equation provided by Richardson et al. (2002). The photochemical reflectance index (PRI) was estimated from each spectrum using the formula ($R531 - R570)/(R531 + R570$) (Gamon et al. 1997).

Gas exchange measurements

Gas exchange measurements were performed using four LI-6400XT Portable Photosynthesis Systems and one LI-6800 Portable Photosynthesis System (LI-COR, Lincoln, Nebraska, USA). Instruments were zeroed using a common nitrogen standard. In the preceding season, light response curves had been performed to determine the saturating irradiance level of 1500 µmol photons m^{-2} s^{-1} for *Q. coccinea* (Burnett et al. 2019). The leaf temperature was controlled during measurement and the set point was determined by the ambient temperature and humidity inside

136 the laboratory at the time of measurement (the temperature ranged from 22-28 °C). Leaves were
137 inserted into the instrument leaf chamber and underwent full acclimation to saturating light (up to
138 90min) until both A and g_s had reached steady-state. A–C_i curves were performed as described
139 previously, using 14 values of C_i (Rogers et al. 2017, Burnett et al. 2019). Values of $V_{c,max}$ and J_{max}
140 were first obtained by fitting the A–C_i curves using the parameters defined by Bernacchi et al.
141 (Bernacchi et al. 2001, Bernacchi et al. 2013, Rogers et al. 2017). Values of $V_{c,max}$ and J_{max} were then
142 normalised to 25 °C with an Arrhenius temperature scaling function using activation energies
143 provided by Bernacchi et al. (2001, 2003), to give $V_{c,max.25}$ and $J_{max.25}$. Efforts to increase
144 representation of $V_{c,max}$ using survey-style measurements of photosynthesis to increase the
145 availability of data from existing databases or to increase the throughput of data collection are not
146 always reliable if leaves were not light-acclimated prior to measurement (De Kauwe et al. 2016,
147 Burnett et al. 2019). Therefore, whilst being more time consuming to perform than a survey-style
148 measurement, A–C_i curves remain the gold-standard approach for measuring photosynthetic
149 capacity. Our analysis is based on C_i rather than C_c and therefore does not account for mesophyll
150 conductance. Thus reported photosynthetic parameters should be considered as apparent.
151
152 Gas exchange measurements were used to derive photosynthetic water use efficiency (WUEi) and
153 photosynthetic nitrogen use efficiency (NUE). WUEi is light-acclimated steady-state A_{sat}/g_s obtained
154 from the first point of each A–C_i curve. NUE is $V_{c,max.25}$/N, both expressed on a mass basis; mass-
155 based $V_{c,max}$ was first obtained from area-based $V_{c,max.25}$ and LMA.
156
157 Gas exchange measurements were also used to calibrate the conductance model needed for
158 modelling photosynthesis. To obtain the stomatal slope parameter g_1, which is the slope of the

relationship between A and g_s and is required for modelling photosynthesis as outlined below, the first point of each A–C_i curve was recorded after initial stabilisation of A and g_s and acclimation to ambient conditions inside the leaf cuvette. For each measurement date, the first points from all A–C_i curves were pooled and the g_1 parameter from the simplified linear USO model (Eq. 1) was obtained using a linear regression as shown previously (Medlyn et al. 2011, Lin et al. 2015, Wu et al. 2020), using a default g_0 of 0:

$$g_{sw} = g_0 + g_1 \frac{1.6\, A_n}{C_s \sqrt{D_s}} \quad \text{Eq. 1}$$

where g_{sw} is the stomatal conductance to water vapor, g_0 and g_1 the intercept and the slope of the linear regression, A_n is net CO_2 assimilation, C_s is CO_2 at the surface of the leaf (C_a) and D_s is leaf to air VPD. For the first measurement date, a good estimate of g_1 could not be obtained so the mean g_1 from all other dates (except the final date for which g_1 was much higher than on all preceding dates) was used instead.

Leaf structural and nitrogen trait measurements

Following the completion of each A–C_i curve, discs of known area were punched from across the leaf surface, including the area used for gas exchange and excluding the prominent lower midrib (Fig. 1c). Leaf discs were weighed, then dried at 70 °C for several days to achieve constant mass. Dried leaves were re-weighed, and relative water content (RWC) and leaf mass per unit area (LMA) were calculated. Dried leaves were subsequently ground, and elemental nitrogen was quantified using a 2400 Series II CHN analyser following the manufacturer's instructions (PerkinElmer, Waltham, MA, USA).

Data analysis

All data analysis was performed within the R open-source software environment (R Core Team 2019). For analysis of each leaf trait (Figs. 3, 4), a one-way repeated measures ANOVA was performed to examine effects over time, with the individual tree as the Error term. A post-hoc Tukey test was then performed to examine pairwise comparisons between each possible pair of measurement dates. When required, data were log- or square-root-transformed prior to analysis as appropriate.

Modelling photosynthesis

Photosynthesis at the top of the canopy was modelled for each measurement date using the *f.AT* function within the 'Leaf Gas Exchange' package in R (https://github.com/TESTgroup-BNL/LeafGasExchange/releases/tag/v1.0). This function simulates photosynthesis using the simplified USO model coupled with the FvCB assimilation model and a leaf energy budget (Muir 2019). The inputs to the model are the ambient atmospheric weather conditions surrounding the leaves (photosynthetically active radiation, air temperature, CO_2 concentration at the leaf surface, wind speed, and relative humidity), the photosynthetic parameters R_d, $V_{c,max.25}$, $J_{max.25}$, and the conductance parameters g_0 and g_1. The outputs are A, g_{sw}, C_i and T_{leaf}. The function *f.AT* was parameterised using $V_{c,max.25}$, $J_{max.25}$, g_0 and g_1 calibrated using the data from this study. For the other parameters necessary to calculate photosynthesis, including R_d, the default parameters used in the Functionally Assembled Terrestrial Ecosystem Simulator (FATES) (Koven et al. 2020) for C_3 plant species were chosen. The weather input variables were set to the mean weather data measured during the week of each sampling date (measurement date ± 3 days) during the 6 hour period around solar noon (10:00-16:00 BST), and CO_2 at the leaf surface was set to 400 µmol mol^{-1}.

Results

Leaf structural traits

Relative water content (RWC) and leaf mass per unit area (LMA) showed inverse relationships to each other (Fig. 3). RWC was initially very high, declined in the middle of the season, and then increased towards the end of the season; LMA was initially very low, increased towards the middle of the season, and declined again at the end of the season. In each case, trait values differed significantly over time (RWC $F_{(6,30)} = 185.8$, $P < 0.001$; LMA $F_{(7,35)} = 11.1$, $P < 0.001$). Pairwise comparisons revealed a significant difference in RWC between all possible measurement date pairs with the exception of the pairs DOY 165-177 (stabilisation of RWC around the solstice), 254-303 and 268-303 (stabilisation at the end of the season). For LMA, there was a significant difference for the following pairs of measurement dates: DOY 149-165, 149-177, 149-206, 149-233, 149-254, 149-268, 165-206, 206-233, 206-303, and 254-303, in line with the strong and significant increase at the beginning of the season, a dip between DOY 206-233, and the decline towards the end of the season. The reporting format 'DOY1'-'DOY2' used here indicates a significant difference between the two named DOYs and does not refer to a date range.

Leaf nitrogen and chlorophyll

When expressed on a leaf mass basis, nitrogen concentration was initially high, was stable throughout much of the season and then gradually declined over the last three measurement dates (Fig. 3). When expressed on a leaf area basis, nitrogen showed a steady increase followed by a steady decrease, with a sharp decline to the final time point, closely following the trend in LMA (Fig. 3). Leaf chlorophyll and photochemical reflectance index (PRI) showed similar trends to nitrogen

per unit area (Fig. 3). Trends in each trait showed significant effects of time (mass-based nitrogen $F_{(7,35)} = 20.1$, $P < 0.001$; area-based nitrogen $F_{(7,35)} = 10.2$, $P < 0.001$; chlorophyll $F_{(7,35)} = 15.3$, $P < 0.001$; PRI $F_{(7,35)} = 14.0$, $P < 0.001$). For mass-based nitrogen, significant differences were observed for the date pairs 149-254, 149-268, and between the final measurement date (DOY 303) and each preceding date. For area-based nitrogen, significant differences were observed between DOY 149-206 and between the final measurement date (DOY 303) and each preceding date, with the exception of DOY 149-303 which did not differ significantly. For chlorophyll, there was a significant difference between the first measurement date (DOY 149) and all subsequent dates with the exception of DOY 303, and there was a significant difference between the final measurement date (DOY 303) and each of the preceding dates with the exception of DOY 149. For PRI there were significant differences between DOY 303 and each of the preceding dates.

Photosynthetic traits

The derived photosynthetic parameters $V_{c,max.25}$, $J_{max.25}$ and light-acclimated net photosynthetic rate A_{sat} showed similar trends (Fig. 4) with a significant effect of time in each case ($V_{c,max.25}$ $F_{(6,29)} = 5.2$; $P < 0.001$, $J_{max.25}$ $F_{(6,26)} = 4.2$, $P < 0.01$; A_{sat} $F_{(6,29)} = 3.7$, $P < 0.01$). These parameters all showed a late season peak (at the penultimate measurement date), followed by a sharp decline. The decline in $J_{max.25}$ between the penultimate and final time points was less marked (41%) than the equivalent decline in $V_{c,max.25}$ (55%). Stomatal conductance (g_s) measured following full acclimation to saturating irradiance, i.e. immediately prior to measuring the A–C_i response followed the same pattern as $V_{c,max.25}$, $J_{max.25}$, and A_{sat} for most of the season (g_s $F_{(6,29)} = 4.7$, $P < 0.01$), but was decoupled at the final time point which showed a very low value of A_{sat} compared to g_s (Fig. 4). This trend is reflected in instantaneous water use efficiency (WUEi) which was at the minimum at the

final time point due to a low rate of A_{sat} compared to g_s (Fig. 4). In contrast, photosynthetic nitrogen use efficiency (NUE) remained relatively constant throughout the measurement period, with the greatest value at the penultimate measurement date coinciding with the late-season peak in photosynthesis (Fig. 4). Both WUEi and NUE displayed significant time effects (WUEi $F_{(6,29)} = 16.0$, $P < 0.001$; NUE $F_{(6,29)} = 4.5$, $P < 0.01$).

Pairwise comparisons made between all pairs of measurement dates revealed significant differences in $V_{c,max.25}$ between DOY 165-254, 254-268, 254-303 and 268-303 highlighting the late-season peak on DOY 268 and dramatic decline at the end of the season. Differences in $J_{max.25}$ were significant between DOY 254-268 and 254-303; differences in A_{sat} were significant between DOY 165-254, 254-268 and 254-303; differences in g_s were significant between DOY 165-254, 165-268, 165-303; in each case these significant differences relate to the late-season peak and subsequent decline described above. Differences in WUEi were significant between DOY 165-233, 165-254 and 165-268 showing the decline from the maximum just before the summer solstice, and between the final measurement date (DOY 303) and each preceding date indicating the sharp decrease in WUE at the end of the season compared to all other dates. Differences in NUE were significant between DOY 165-254 and 254-303.

Modelling photosynthesis

Using ambient environmental conditions from the week of measurement (measurement date ± 3 days) during the 6 hour period around solar noon (10:00-16:00 BST), and modelled values of g_0 and g_1, modelled values of $V_{c,max.25}$ and $J_{max.25}$ were used to predict the rate of net photosynthesis at the

top of the canopy (Fig. 5). Modelled photosynthesis closely matched the trend in $V_{c,max.25}$ – including the steeper decline at the final time point seen for $V_{c,max.25}$ than for $J_{max.25}$ (Fig. 4).

Using the model framework, we further explored how seasonality in parameters could impact the modelling of growing season photosynthesis. We did this by examining the deviation from the mean in both $V_{c,max.25}$ and modelled *A* to explore how seasonal conditions can change the overall canopy-scale photosynthetic carbon update. We found that there was substantial seasonality, and variation increased throughout the season with values both greater and lower than the mean (Fig. 6). In each case the deviation was lowest at and around the midsummer solstice, and greatly increased in magnitude with the late-season peak and end-season decline in photosynthesis (Fig. 6). The maximum deviation from the mean was 41% for $V_{c,max.25}$ and 52% for modelled *A.*

Discussion

We sought to understand seasonal trends in physiological traits of *Q. coccinea*, explore the mechanisms underpinning these trends, and consider the modelling implications of using single time point measurements of photosynthesis to parameterise carbon models. Our results indicate a surprising late-season maximum in photosynthesis coincident with a rise in leaf water content and stomatal conductance, lower air temperatures, and an overall reduction in atmospheric VPD. In contrast to our hypothesis, photosynthetic capacity did not peak at the solstice and displayed significant deviation from the mean value later in the season.

Variability in photosynthetic capacity and rate is related to climate

Photosynthetic traits displayed great variability across the season. Similar to previous studies (e.g. Yang et al. 2016), we observed a typical Gaussian seasonal curve for traits such as pigment content, LMA, and area-based nitrogen, while mass-based nitrogen and RWC generally showed a steady decline from leaf flush to senescence. Contrary to our expectations, and in contrast to the findings of several previous studies demonstrating the seasonal Gaussian trend in photosynthesis that we had expected, with the peak at the summer solstice (Wilson et al. 2000, 2001, Grassi et al 2005, Kosugi and Matsuo 2006, Bauerle et al. 2012), the peak in photosynthetic rate and capacity occurred late in the season, at the penultimate measurement point (Fig. 4). Whilst the amount of daylight was greatest at the midsummer solstice (Fig. 2), with both the highest PAR and the longest daylength combining to give the greatest integrated daily light levels, this did not coincide with maximal photosynthetic rate. Rather, the peak in $V_{c,max.25}$, $J_{max.25}$ and A_{sat} occurred once the high summer temperatures and VPD began to decline yet before daily PAR decreased (Figs. 2, 4). This coincided with an increase in RWC (Fig. 3) which followed the peak summer heat (Fig. 2). Whilst the year of measurement was slightly warmer and drier than some previous years, it was not exceptional in terms of meteorological factors (see Figure S1 available as Supplementary Data at *Tree Physiology* Online). A previous study in which *Q. douglasii* (blue oak) was exposed to heat stress revealed a strong effect of heat on $V_{c,max.25}$; this study also showed a slight end of season peak in $V_{c,max.25}$ prior to senescence although this was not the seasonal maximum (Xu and Baldocchi 2003).

RWC and LMA were generally inversely correlated with one another (Fig. 3). At the start of the season, RWC was at its highest and LMA at its lowest as the developing leaves were thin, soft and

not fully expanded at the first measurement date which was within a couple of weeks of leaf flushing. After the solstice, as temperatures increased, RWC declined, and recovered later in the season as temperatures declined (Figs. 2, 3). LMA, conversely, was high during the middle of the season where leaves were structurally mature, and declined at the end, in accordance with studies demonstrating a positive correlation between leaf age and LMA during the growing season prior to senescence (Grassi et al. 2005, Wright et al. 2006, Hikosaka et al. 2007).

The seasonal change in photosynthesis seen here appears to be driven by climatic factors rather than photoperiod. The lower temperatures and VPD, accompanied by higher RWC, are correlated with an increase in g_s and increased photosynthetic rate and capacity enabling *Q. coccinea* to maximise carbon gain in advance of leaf senescence and over-wintering (Figs. 2, 3, 4). Relationships between the meteorological data and $V_{c,max.25}$ presented in this study are shown in Figure S2 (available as Supplementary Data at *Tree Physiology* Online). Several previous studies have demonstrated strong effects of environmental factors on photosynthesis, in a range of species (e.g. Ellsworth 2000, Grassi 2005, Choat et al. 2006, Kosugi and Matsuo 2006). These responses vary between species; for example, a comparison of evergreen and deciduous species in Australia highlighted the greater sensitivity of photosynthesis in deciduous trees to dryness (Choat et al. 2006). Furthermore, it should be noted that in addition to seasonal trends in environmental factors throughout the growing season, the environment at the time of leaf flushing can also impact physiological processes (Wujeska-Klause et al. 2019).

342 *Leaf senescence is accompanied by a strong decline in photosynthesis*

343 Leaf age effects, in addition to environmental factors, vary during the growing season, with nutrient
344 resorption being a key process affecting photosynthetic activity at the time of leaf senescence
345 (Crous et al. 2019); ontogenetic effects impact photosynthesis throughout leaf development (Field
346 and Mooney 1983, Ellsworth 2000, Jach and Ceulemans 2000, Grassi et al. 2005, Kosugi and Matsuo
347 2006, Wright et al. 2006, Hikosaka et al. 2007, Greenwood et al. 2008). In the present study,
348 between the penultimate and final time points, PAR and temperature decreased dramatically (Fig.
349 2), accompanied by a sharp decrease in nitrogen, chlorophyll and PRI (Fig. 3). Although values of
350 RWC and g_s displayed relatively little change between the penultimate and the final time point
351 (Figs. 3, 4), A_{sat} decreased sharply between the last two measurement dates leading to a decoupling
352 of A_{sat} and g_s and a strong decrease in WUEi (Fig. 4). The decrease in A_{sat} was accompanied by a
353 sharp decline in $V_{c,max.25}$ and $J_{max.25}$ (Fig. 4). The decline in $V_{c,max.25}$ was relatively greater than the
354 decline in $J_{max.25,}$which did not drop below its previous lowest value. This might reflect the greater
355 dependency of $V_{c,max.25}$ than $J_{max.25}$ on leaf nitrogen content, which decreased greatly at the final
356 time point in line with the onset of nutrient resorption and leaf senescence (Fig. 4). Moreover, leaf
357 ontogeny interacts with the environment. An example of this interaction is that older leaves may be
358 less susceptible to drought; one study demonstrated that year-old leaves of the evergreen loblolly
359 pine were less affected by drought than new leaves and reached peak photosynthetic capacity
360 earlier in the year (Ellsworth 2000), whilst a study of deciduous trees showed that the Gaussian
361 trend in photosynthesis associated with changing leaf age and environmental conditions
362 throughout the season persisted but with a reduced photosynthetic capacity, during conditions of
363 summer drought (Grassi et al. 2005).

364

Photosynthetic nitrogen use efficiency is maintained throughout the season

Photosynthetic NUE remained fairly constant throughout the measurement season, with the exception of the penultimate time point (Fig. 4). The lowest NUE coincided with the lowest photosynthesis, during the hottest and driest part of the season, at which point *A* decreased whilst nitrogen remained stable, a trend which has been reported previously in the mid to late summer (Wilson et al. 2001). At the penultimate time point, photosynthetic rate and capacity increased significantly whilst nitrogen remained very similar compared to the preceding measurement (Figs. 3, 4) leading to a peak in NUE. This may be underpinned by the lower ambient air temperatures and lower VPD facilitating increases in RWC and g_s, allowing A_{sat} to increase (Figs. 2, 3, 4). At the end of the season, values of both photosynthesis and nitrogen were very low due to the remobilisation of nitrogen resources during senescence; this remobilisation means that photosynthetic NUE did not decrease despite the low rate and capacity of photosynthesis (Figs. 3, 4).

Trends in nitrogen varied depending on whether nitrogen was expressed per unit mass or per unit area (Fig. 3), due to the changing relationship between leaf mass and area seen in the LMA data. At the start of the season, leaves had a low LMA and therefore a low amount of nitrogen per unit area (Fig. 3), as has been found previously (Grassi et al. 2005, Wright et al. 2006, Hikosaka et al. 2007). However, the nitrogen concentration per unit mass was at its highest at the first measurement (Fig. 3), as seen elsewhere (Yang et al. 2016) since leaf growth was concurrent with assembly of the photosynthetic machinery despite full leaf expansion not having been achieved. Chlorophyll, PRI and nitrogen content mimicked the trend in LMA to a large extent and this was especially the case for nitrogen (Fig. 3). However, this relationship was decoupled at the final time point. Whilst chlorophyll and nitrogen dropped sharply to their lowest levels due to the nutrient remobilisation

processes of leaf senescence, LMA did not decline so steeply. The tight link between nitrogen and chlorophyll (when nitrogen is expressed on a leaf area basis) likely reflects the coupling between chlorophyll for light harvesting and nitrogen for the enzymes of the Calvin-Benson cycle (in particular, Rubisco).

Implications for modelling photosynthesis

Modelled photosynthesis at the top of the canopy closely reflected $V_{c,max.25}$ indicative of Rubisco limited (or RuBP saturated) photosynthesis throughout the season (Figs. 4, 5). In order to understand the constraints associated with selecting a time point for deriving model parameters, we plotted the deviation in $V_{c,max.25}$ and modelled *A* for each measurement date (Fig. 6). In each case, values early in the season, before and around the midsummer solstice, led to lower deviation from the mean than values later in the season (Fig. 6). This is due to the late season peak in photosynthesis occurring before the end of season decline, which contributes large deviations in $V_{c,max.25}$ and modelled *A*. In our analysis, these trends in photosynthetic parameters mean that we did not observe a peak in $V_{c,max.25}$ and modelled *A* at the solstice followed by a decline; these findings therefore contrast with our hypothesis that a measurement around the solstice would lead to a large deviation from the seasonal mean. In this instance, an early-season or midsummer solstice measurement would be most appropriate for deriving a seasonal mean value of $V_{c,max.25}$ or modelled *A* for use in carbon cycle models. Whilst additional years of measurement are required to confirm the trend reported here, alongside continued integration of theory and practice, the surprising variation in photosynthetic capacity and rate uncovered here for *Q. coccinea* highlights the necessity of understanding the species-level and ecosystem-level responses of photosynthesis to seasonal change if accurate estimates of photosynthetic parameters are to be obtained.

411

412 Environmental conditions therefore play an important role in modulating seasonal trends in $V_{c,max.25}$
413 with a clear need to account for seasonality (Jiang et al. 2020). Whilst climate shapes
414 photosynthetic capacity along optimality principles (Smith et al. 2019), variation gradients also
415 impact physiological processes at the seasonal scale. Furthermore, environmental factors such as
416 temperature and water availability interact with leaf ontogeny, meaning that the biological
417 processes occurring within the plant such as leaf expansion impact the extent to which external
418 parameters affect photosynthesis (Grassi et al. 2005, Kosugi and Matsuo 2006). We advocate
419 moving away from the need to establish a seasonal mean value of $V_{c,max.25}$, towards a greater
420 understanding of the factors driving seasonality in $V_{c,max.25}$. This may then be replicated in models to
421 increase the accuracy of representation of photosynthetic capacity across seasons and years under
422 different climatic conditions and across geographical areas.

423

424 *Conclusions*

425 We hypothesised that photosynthetic rates and capacities would be greatest at the midsummer
426 solstice. Our findings run contrary to this hypothesis, with the greatest values of $V_{c,max.25}$, $J_{max.25}$ and
427 A_{sat} observed at the penultimate measured time point, in late September. Contrary to our
428 expectations, a measurement of photosynthetic traits in *Q. coccinea* taken at or around the summer
429 solstice provides the closest estimate to the mean seasonal value and is therefore the most suitable
430 time point for deriving model parameters for this species. However, we recommend incorporating
431 seasonality in models for the most accurate representation. A multi-year, multi-species approach is
432 needed to validate the trends shown here, yet our findings clearly indicate the potential for
433 deviation from expected trends. A mid to late-season measurement of photosynthesis could lead to

434 a dramatic over- or under-estimation of $V_{c,max.25}$ or modelled A, resulting in significant impacts in
435 subsequent ecosystem modelling. Species- and environment-specific consideration, alongside
436 consideration of leaf ontogeny, is necessary for accurate modelling of seasonal carbon uptake in
437 deciduous forests.

Data and Materials Availability

All data associated with this manuscript are publically available at the DOI listed in 'Supplementary data'.

Supplementary data

Figure S1. Ten-year meteorological data.

Figure S2. Relationships between physiological and meteorological data.

Supplementary Dataset. The data presented in this manuscript are available on-line [http://ecosis.org] from the Ecological Spectral Information System (EcoSIS). DOI 10.21232/ujBYNxhm

Conflict of interest

None declared.

Funding

United States Department of Energy contract DE-SC0012704 to Brookhaven National Laboratory.

Acknowledgements

We gratefully acknowledge Duncan Anderson, Sophie Drew, Casey Hamilton, Benjamin Miller and Ivanellis Rodriguez-Torres for assistance with data collection.

Authors' Contributions

ACB, SPS and AR conceived and designed the study. All authors contributed to methodology development, experiment execution and data collection. ACB analysed the data and wrote the manuscript with contributions from SPS, JL and AR.

References

Ali AA, Xu C, Rogers A, McDowell NG, Medlyn BE, Fisher RA, Wullschleger SD, Reich PB, Vrugt JA, Bauerle WL, Santiago LS, Wilson CJ (2015) Global-scale environmental control of plant photosynthetic capacity. Ecol Appl 25:2349–2365.

Bauerle WL, Oren R, Way DA, Qian SS, Stoy PC, Thornton PE, Bowden JD, Hoffman FM, Reynolds RF (2012) Photoperiodic regulation of the seasonal pattern of photosynthetic capacity and the implications for carbon cycling. Proc Natl Acad Sci U S A 109:8612–8617.

Bernacchi CJ, Singsaas EL, Pimentel C, Portis Jr AR, Long SP (2001) Improved temperature response functions for models of Rubisco-limited photosynthesis. Plant Cell Environ 24:253-259.

Bernacchi CJ, Pimentel C, Long SP (2003) In vivo temperature response functions required to model RuBP-limited photosynthesis. Plant Cell Environ 26:1419-1430.

Bernacchi CJ, Bagley JE, Serbin SP, Ruiz-Vera UM, Rosenthal DM, Vanloocke A (2013) Modelling C3 photosynthesis from the chloroplast to the ecosystem. Plant, Cell Environ 36:1641–1657.

Burnett AC, Davidson KJ, Serbin SP, Rogers A (2019) The “one-point method” for estimating maximum carboxylation capacity of photosynthesis: A cautionary tale. Plant Cell Environ 42:2472–2481.

Choat B, Ball MC, Luly JG, Donnelly CF, Holtum JAM (2006) Seasonal patterns of leaf gas exchange and water relations in dry rain forest trees of contrasting leaf phenology. Tree Physiol

26:657-664.

Crous KY, Wujeska-Klause A, Jiang MK, Medlyn BE, Ellsworth DS (2019) Nitrogen and phosphorus retranslocation of leaves and stemwood in a mature *Eucalyptus* forest exposed to 5 years of elevated CO_2. Front Plant Sci 10:13.

Ellsworth DS (2000) Seasonal CO_2 assimilation and stomatal limitations in a *Pinus taeda* canopy. Tree Physiol 20:435-445.

Field C, Mooney HA (1983) Leaf age and seasonal effects on light, water, and nitrogen use efficiency in a California shrub. Oecologia 56:348-355.

Gamon JA, Serrano L, Surfus JS (1997) The photochemical reflectance index: An optical indicator of photosynthetic radiation use efficiency across species, functional types, and nutrient levels. Oecologia 112:492–501.

Grassi G, Vicinelli E, Ponti F, Cantoni L, Magnani F (2005) Seasonal and interannual variability of photosynthetic capacity in relation to leaf nitrogen in a deciduous forest plantation in northern Italy. Tree Physiol 25:349-360.

Greenwood MS, Ward MH, Day ME, Adams SL, Bond BJ (2008) Age-related trends in red spruce foliar plasticity in relation to declining productivity. Tree Physiol 28:225-232.

Hikosaka K, Nabeshima E, Hiura T (2007) Seasonal changes in the temperature response of photosynthesis in canopy leaves of *Quercus crispula* in a cool-temperate forest. Tree Physiol 27:1035-1041.

Jach ME, Ceulemans R (2000) Effects of season, needle age and elevated atmospheric CO_2 on photosynthesis in Scots pine (*Pinus sylvestris*). Tree Physiol 20:145-157.

Jiang C, Ryu Y, Wang H, Keenan T (2020) An optimality-based model explains seasonal variation in C3 plant photosynthetic capacity. Glob Chang Biol:1–18.

Kamoske A, Dahlin K, Serbin S, Stark S (2020) Leaf traits and canopy structure together explain canopy functional diversity: an airborne remote sensing approach. Ecol Appl

Kattge J, Knorr W, Raddatz T, Wirth C (2009) Quantifying photosynthetic capacity and its relationship to leaf nitrogen content for global-scale terrestrial biosphere models. Glob Chang Biol 15:976–991.

De Kauwe MG, Lin YS, Wright IJ, Medlyn BE, Crous KY, Ellsworth DS, Maire V, Prentice IC, Atkin OK, Rogers A, Niinemets Ü, Serbin SP, Meir P, Uddling J, Togashi HF, Tarvainen L, Weerasinghe LK, Evans BJ, Ishida FY, Domingues TF (2016) A test of the 'one-point method' for estimating maximum carboxylation capacity from field-measured, light-saturated photosynthesis. New Phytol 210:1130–1144.

Knauer J, El-Madany T, Zaehle S, Migliavacca M (2018) Bigleaf - An R package for the calculation of physical and physiological ecosystem properties from eddy covariance data. PLoS One 13:doi: 10.1371/journal.pone.0201114.

Kosugi Y, Matsuo N (2006) Seasonal fluctuations and temperature dependence of leaf gas exchange parameters of co-occurring evergreen and deciduous trees in a temperate broad-leaved forest. Tree Physiol 26:1173-1184.

Koven CD, Knox RG, Fisher RA, Fisher RA, Chambers JQ, Chambers JQ, Christoffersen BO, Davies SJ, Detto M, Detto M, Dietze MC, Faybishenko B, Holm J, Huang M, Kovenock M, Kueppers LM, Kueppers LM, Lemieux G, Massoud E, McDowell NG, Muller-Landau HC, Muller-Landau

HC, Needham JF, Norby RJ, Powell T, Rogers A, Serbin SP, Shuman JK, Swann ALS, Swann ALS, Varadharajan C, Walker AP, Joseph Wright S, Xu C (2020) Benchmarking and parameter sensitivity of physiological and vegetation dynamics using the Functionally Assembled Terrestrial Ecosystem Simulator (FATES) at Barro Colorado Island, Panama. Biogeosciences 17:3017–3044.

Lin YS, Medlyn BE, Duursma RA, Prentice IC, Wang H, Baig S, Eamus D, De Dios VR, Mitchell P, Ellsworth DS, De Beeck MO, Wallin G, Uddling J, Tarvainen L, Linderson ML, Cernusak LA, Nippert JB, Ocheltree TW, Tissue DT, Martin-StPaul NK, Rogers A, Warren JM, De Angelis P, Hikosaka K, Han Q, Onoda Y, Gimeno TE, Barton CVM, Bennie J, Bonal D, Bosc A, Löw M, Macinins-Ng C, Rey A, Rowland L, Setterfield SA, Tausz-Posch S, Zaragoza-Castells J, Broadmeadow MSJ, Drake JE, Freeman M, Ghannoum O, Hutley LB, Kelly JW, Kikuzawa K, Kolari P, Koyama K, Limousin JM, Meir P, Da Costa ACL, Mikkelsen TN, Salinas N, Sun W, Wingate L (2015) Optimal stomatal behaviour around the world. Nat Clim Chang 5:459–464.

Long SP, Bernacchi CJ (2003) Gas exchange measurements, what can they tell us about the underlying limitations to photosynthesis? Procedures and sources of error. J Exp Bot 54:2393–401. http://www.ncbi.nlm.nih.gov/pubmed/14512377 (22 May 2013, date last accessed).

Medlyn BE, Duursma RA, Eamus D, Ellsworth DS, Prentice IC, Barton CVM, Crous KY, De Angelis P, Freeman M, Wingate L (2011) Reconciling the optimal and empirical approaches to modelling stomatal conductance. Glob Chang Biol 17:2134–2144.

Meng R, Wu J, Schwager KL, Zhao F, Dennison PE, Cook BD, Brewster K, Green TM, Serbin SP (2017) Using high spatial resolution satellite imagery to map forest burn severity across spatial scales in a Pine Barrens ecosystem. Remote Sens Environ 191:95–109. http://dx.doi.org/10.1016/j.rse.2017.01.016

Muir CD (2019) Tealeaves: An R package for modelling leaf temperature using energy budgets. AoB Plants 11:1–10.

R Core Team (2019) R: A language and environment for statistical computing. R Foundation for Statistical Computing, Vienna, Austria. URL https://www.R-project.org/.

Richardson AD, Duigan SP, Berlyn GP (2002) An evaluation of noninvasive methods to estimate foliar chlorophyll content. New Phytol 153:185–194.

Rogers A, Serbin SP, Ely KS, Sloan VL, Wullschleger SD (2017) Terrestrial biosphere models underestimate photosynthetic capacity and CO2 assimilation in the Arctic. New Phytol 216:1090–1103.

Serbin SP, Singh A, McNeil BE, Kingdon CC, Townsend PA (2014) Spectroscopic determination of leaf morphological and biochemical traits for northern temperate and boreal tree species. Ecol Appl 24:1651–1669.

Smith NG, Keenan TF, Colin Prentice I, Wang H, Wright IJ, Niinemets Ü, Crous KY, Domingues TF, Guerrieri R, Yoko Ishida F, Kattge J, Kruger EL, Maire V, Rogers A, Serbin SP, Tarvainen L, Togashi HF, Townsend PA, Wang M, Weerasinghe LK, Zhou SX (2019) Global photosynthetic capacity is optimized to the environment. Ecol Lett 22:506–517.

USDA (2019) Fire Effects Information System. https://www.feis-crs.org/feis/

Wang Q, Iio A, Kakubari Y (2008) Broadband simple ratio closely traced seasonal trajectory of canopy photosynthetic capacity. Geophys Res Lett 35:1–5.

Wilson KB, Baldocchi DD, Hanson PJ (2000) Spatial and seasonal variability of photosynthetic parameters and their relationship to leaf nitrogen in a deciduous forest. Tree Physiol 20:565–578.

Wilson KB, Baldocchi DD, Hanson PJ (2001) Leaf age affects the seasonal pattern of photosynthetic capacity and net ecosystem exchange of carbon in a deciduous forest. Plant, Cell Environ 24:571–583.

Wright IJ, Leishman MR, Read C, Westoby M (2006) Gradients of light availability and leaf traits with leaf age and canopy position in 28 Australian shrubs and trees. Funct Plant Biol 33:407-419.

Wu J, Rogers A, Albert LP, Ely K, Prohaska N, Wolfe BT, Oliveira RC, Saleska SR, Serbin SP (2019) Leaf reflectance spectroscopy captures variation in carboxylation capacity across species, canopy environment and leaf age in lowland moist tropical forests. New Phytol 224:663–674.

Wu J, Serbin SP, Ely KS, Wolfe BT, Dickman LT, Grossiord C, Michaletz ST, Collins AD, Detto M, McDowell NG, Wright SJ, Rogers A (2020) The response of stomatal conductance to seasonal drought in tropical forests. Glob Chang Biol 26:823–839.

Wujeska-Klause A, Crous KY, Ghannoum O, Ellsworth DS (2019) Lower photorespiration in elevated CO_2 reduces leaf N concentrations in mature *Eucalyptus* trees in the field. Glob Change Biol 25:1282-1295.

Xu L, Baldocchi DD (2003) Seasonal trends in photosynthetic parameters and stomatal conductance of blue oak (Quercus douglasii) under prolonged summer drought and high temperature. Tree Physiol 23:865–877.

Yang X, Tang J, Mustard JF, Wu J, Zhao K, Serbin S, Lee JE (2016) Seasonal variability of multiple leaf traits captured by leaf spectroscopy at two temperate deciduous forests. Remote Sens Environ 179:1–12. http://dx.doi.org/10.1016/j.rse.2016.03.026

List of Figures

Figures

Figure 1. Shotgun sampling technique for retrieving leaf samples of *Q. coccinea*. (a) A shotgun was used to obtain a sample from the top of the canopy. (b) Stems were re-cut underwater and samples stored on the forest floor until sample collection was complete. (c) Following physiological data collection, leaf discs were punched out of the leaf; discs were used in subsequent measurements of structural traits and leaf nitrogen.

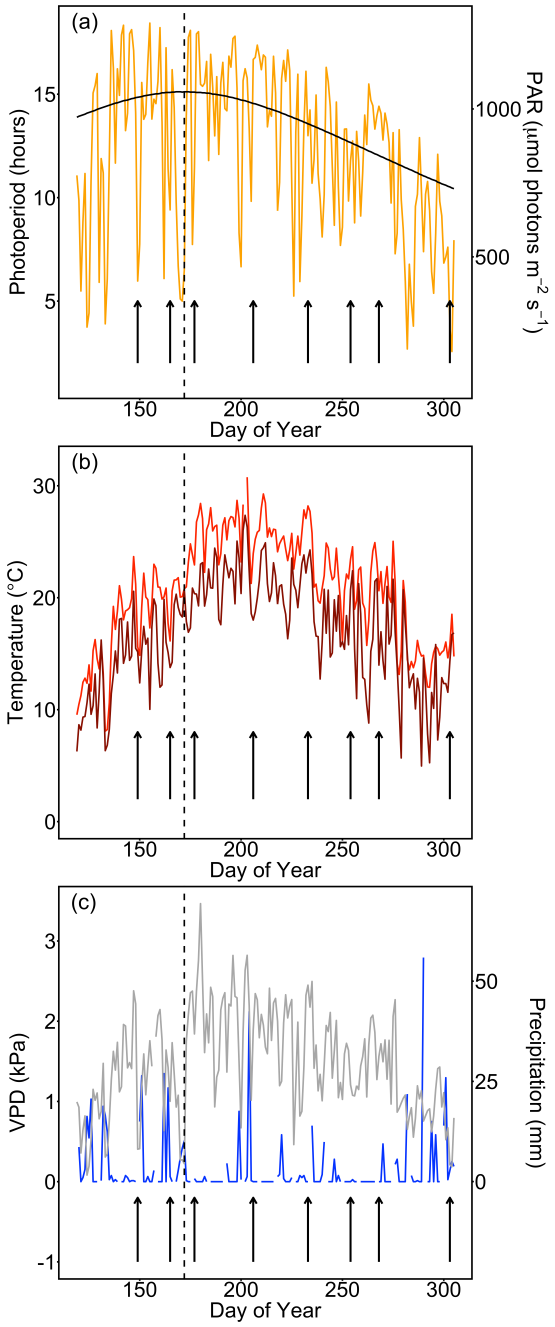

Figure 2. Meteorological data throughout the sampling period, beginning 30 days before the first measurement. Sampling dates are indicated with vertical black arrows and the midsummer solstice is indicated with a vertical black dashed line. (a) Photoperiod (solid black line; primary *y*-axis) and mean daytime photosynthetically active radiation on each measurement date (PAR; yellow line; secondary *y*-axis). (b) Mean daytime temperature (bright red line) and nighttime temperature (dark red line). (c) Maximum daily vapour pressure deficit (VPD; grey line; primary *y*-axis) and total daily precipitation (bright blue line; secondary *y*-axis).

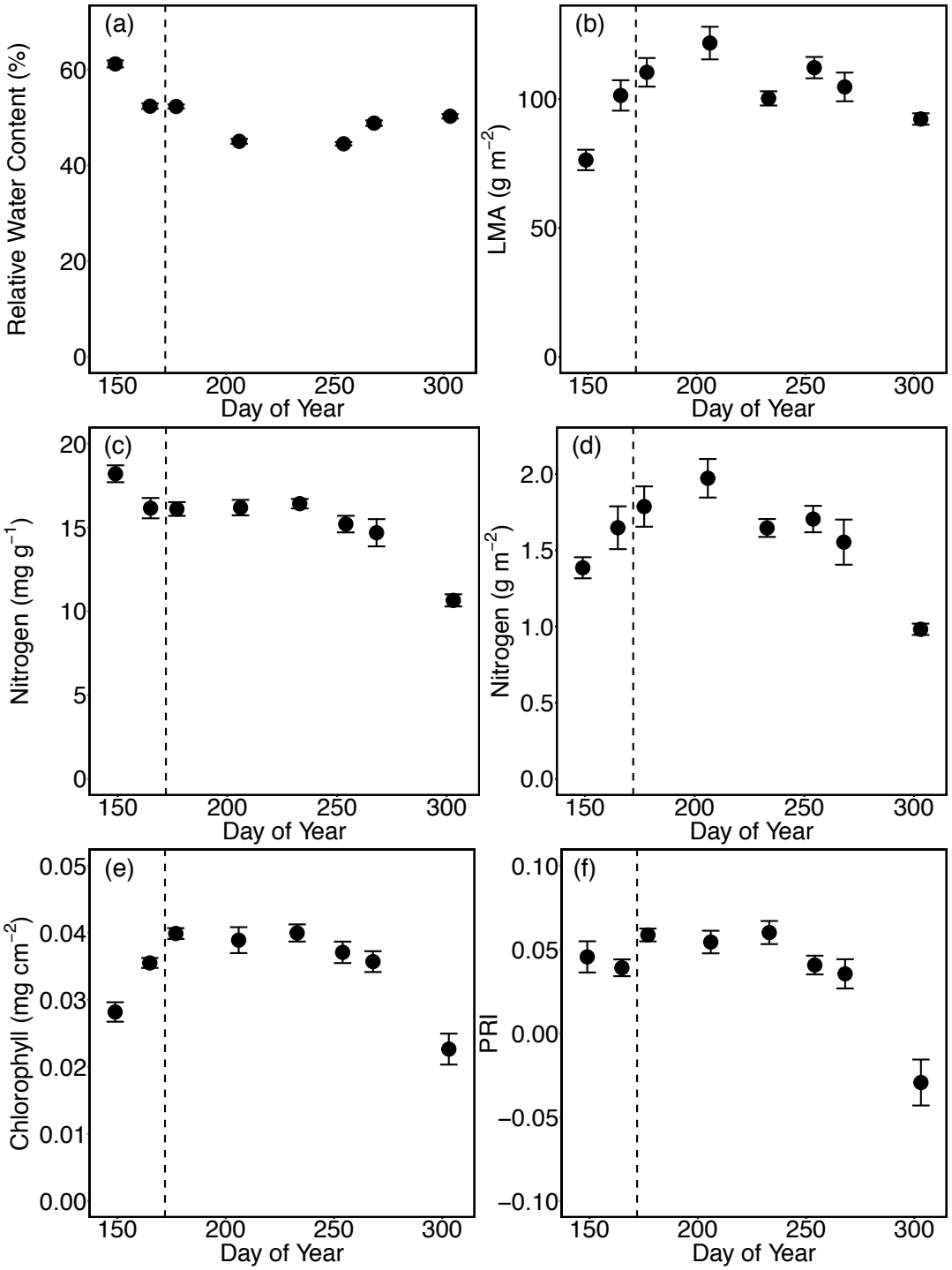

Figure 3. Seasonal trends in leaf structural traits, nitrogen, chlorophyll, and photochemical reflectance index. The midsummer solstice is indicated with a dashed line. (a) relative water content, RWC; (b) leaf mass per unit area, LMA; (c) leaf nitrogen concentration per gram; (d) leaf nitrogen content per m^2; (e) chlorophyll estimated using a leaf reflectance index; (f) photochemical reflectance index, PRI. Plots show mean ±SE, n=6 trees.

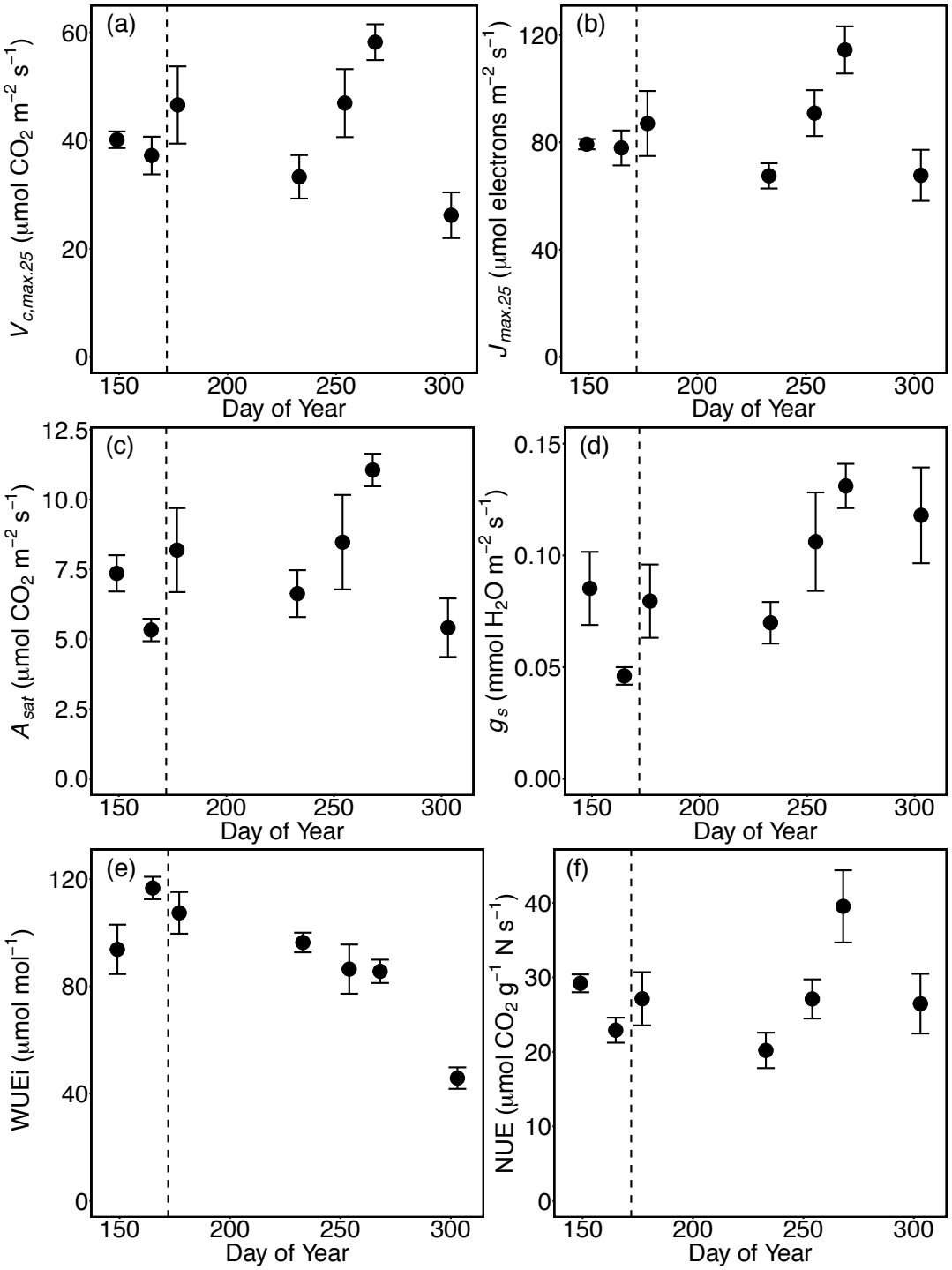

Figure 4. Seasonal trends in photosynthetic traits. The midsummer solstice is indicated with a dashed line. (a) Maximum carboxylation capacity of Rubisco normalised to 25 °C, $V_{c,max.25}$; (b) maximum electron transport rate normalised to 25 °C, $J_{max.25}$; (c) light-saturated photosynthesis, A_{sat}, measured immediately prior to the A–C_i curve; (d) light-acclimated stomatal conductance, g_s, measured immediately prior to the A–C_i curve; (e) instantaneous water use efficiency, WUEi; (f) nitrogen use efficiency of photosynthesis, NUE. Plots show mean ±SE, n=6 trees.

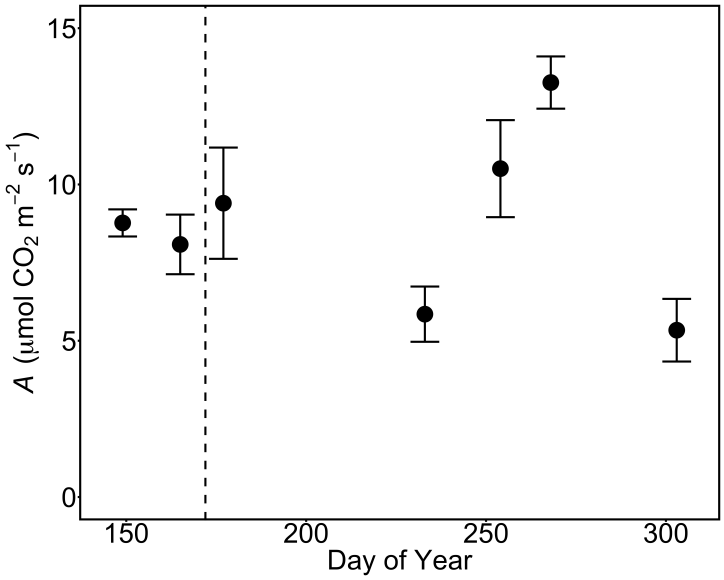

Figure 5. Photosynthesis (*A*) at the top of the canopy modelled from environmental data, photosynthetic capacity and stomatal slope parameters. The midsummer solstice is indicated with a dashed line. Plots show mean ±SE, n=6 trees.

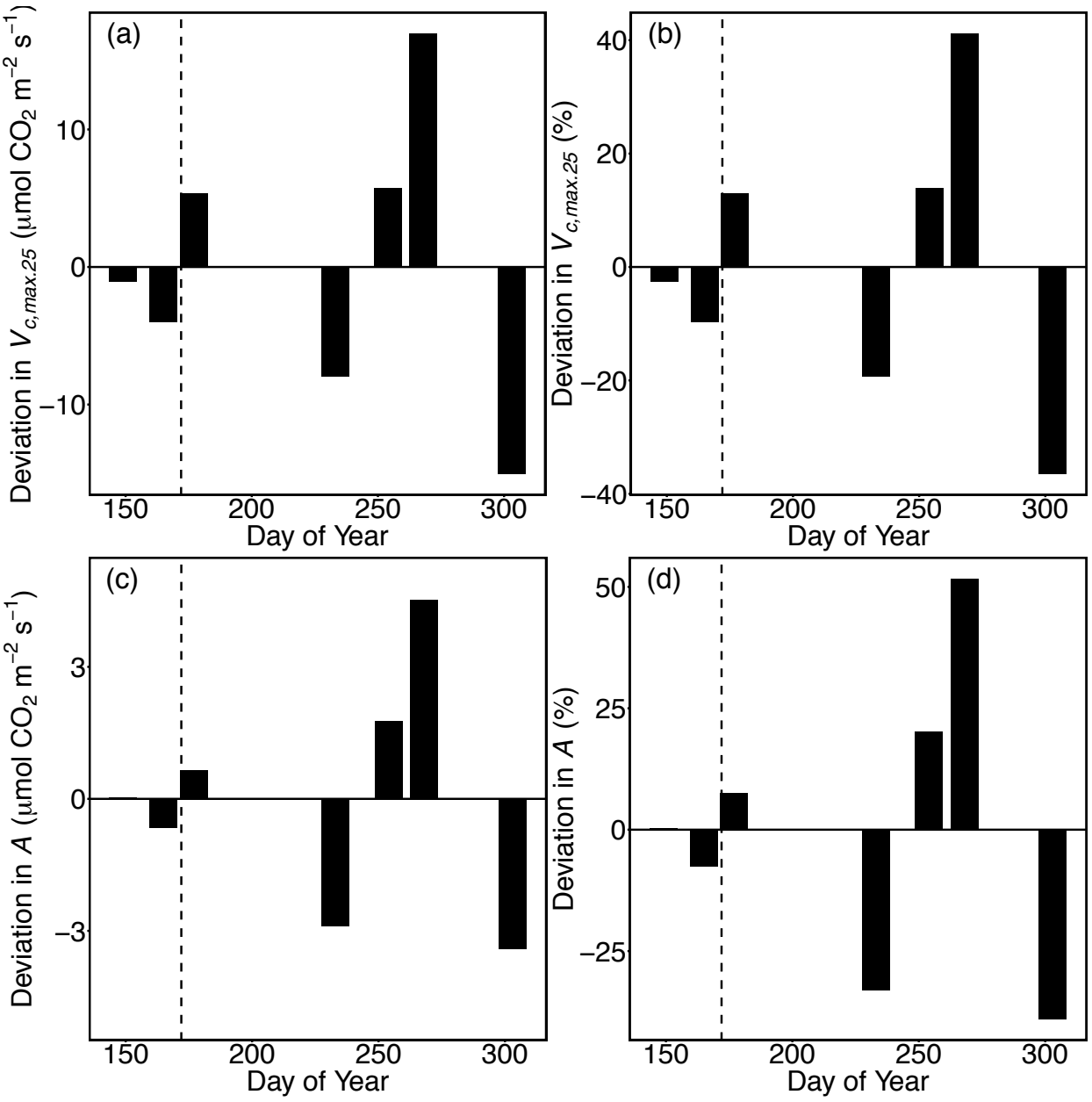

Figure 6. Both the maximum carboxylation capacity of Rubisco ($V_{c,max.25}$) and modelled photosynthesis (A) at the top of the canopy deviate from the mean, with deviation increasing as the measurement season progresses. The horizontal black line (y = 0) indicates the mean value of $V_{c,max.25}$ or A. The midsummer solstice is indicated with a dashed line. (a) Absolute deviation in $V_{c,max.25}$; (b) percentage deviation in $V_{c,max.25}$; (c) absolute deviation in modelled A; (d) percentage deviation in modelled A.

Supplementary Information – Burnett et al.

Figure S1. Ten-year trends in meteorological data at the study site, with the final year shown (2019) being the year in which the study was performed. Note that no solar data were available for the year 2010. Each point shows the average across a 24-hour period.

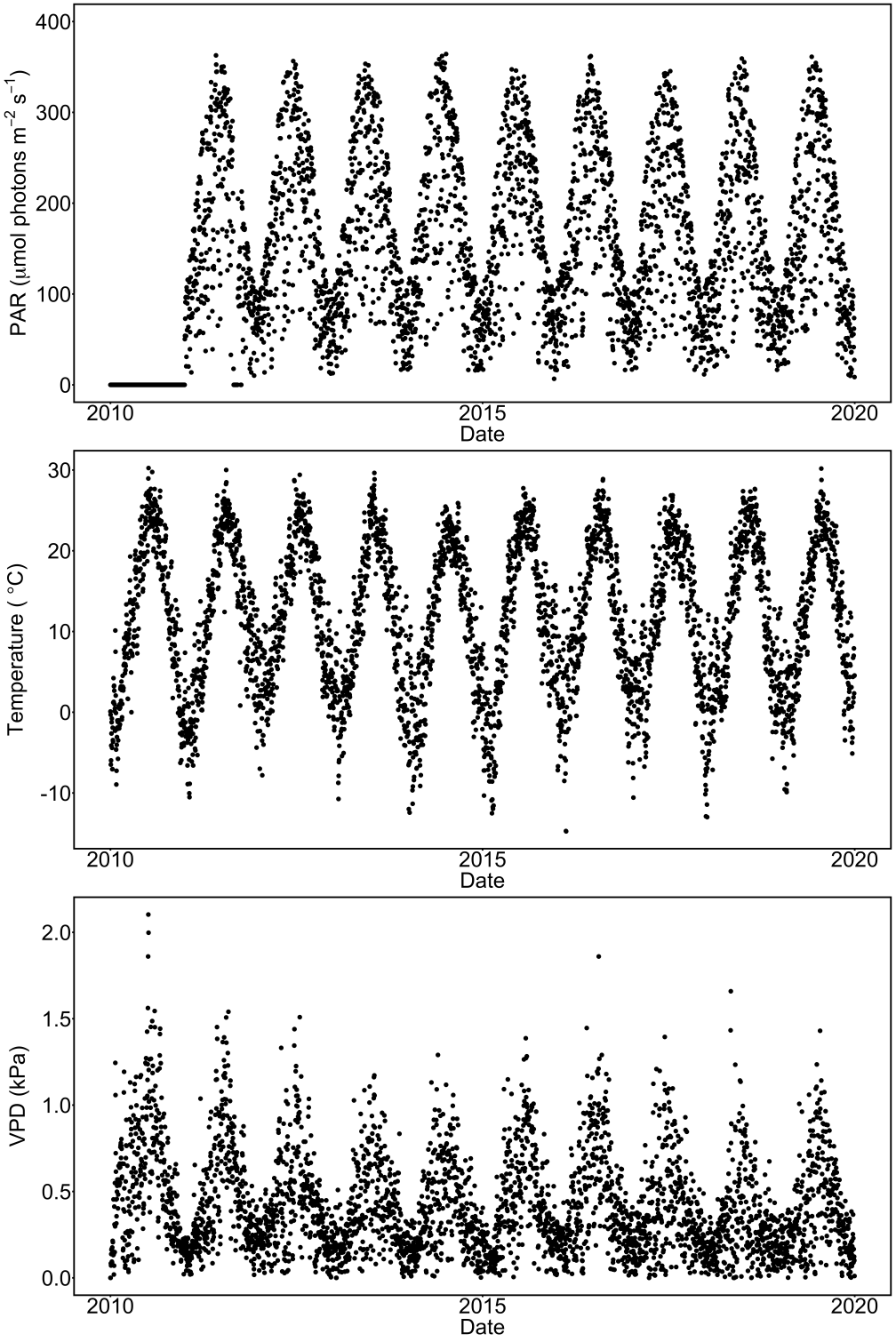

Figure S2. Relationships between the maximum carboxylation capacity of Rubisco ($V_{c,max.25}$) and the meteorological data on dates of measurement. For detailed descriptions of the parameters refer to the legend for Figure 2 within the main manuscript.